Wave-number–frequency spectrum for turbulence from a random sweeping hypothesis with mean flow

M. Wilczek and Y. Narita

Phys. Rev. E **86**, 066308 — Published 13 December 2012
DOI: 10.1103/PhysRevE.86.066308

Wavenumber-frequency spectrum for turbulence from a random sweeping hypothesis with mean flow

M. Wilczek[1,*] and Y. Narita[2,3]

[1]*Institute for Theoretical Physics, University of Münster, Wilhelm-Klemm-Str. 9, D-48149 Münster, Germany*
[2]*Space Research Institute, Austrian Academy of Sciences, Schmiedlstraße 6, A-8042 Graz, Austria*
[3]*Institut für Geophysik und extraterrestrische Physik, Technische Universität Braunschweig, Mendelssohnstr. 3, D-38106 Braunschweig, Germany*

(Dated: October 31, 2012)

We derive the energy spectrum in wavenumber-frequency space for turbulent flows based on Kraichnan's idealized random sweeping hypothesis with additional mean flow, which yields the instantaneous energy spectrum multiplied by a Gaussian frequency distribution. The model spectrum has two adjustable parameters, the mean flow velocity and the sweeping velocity, and has the property that the power-law index of the wavenumber spectrum translates to the frequency spectrum, invariant for arbitrary choices of the mean velocity and sweeping velocity. The model spectrum incorporates both Taylor's frozen-in flow approximation and the random sweeping approximation in a natural way, and can be used to distinguish between these two effects when applied to real time-resolved multi-point turbulence data. Evaluated in real space, its properties with respect to space-time velocity correlations are discussed, and a comparison to the recently introduced Elliptic Model is drawn.

I. INTRODUCTION

One main feature of turbulence is the excitation of a broad spectrum of fluctuations observable in most turbulent quantities like the velocity, passive or active scalars and electromagnetic fields. Among the most important statistics characterizing these fluctuating fields are second-order quantities like the energy spectrum or correlation functions. When measuring these quantities in turbulent flows using time-resolved single-point measurements, one faces the challenge to relate temporal fluctuations with spatial ones, as e.g., Kolmogorov's inertial-range spectrum was derived in the wavenumber domain [1]. Two distinct methods or approximations are known in observational turbulence studies that associate frequencies with wavenumbers: One is the frozen-in flow hypothesis proposed by Taylor [2], which assumes that the flow field is advected past the probe with a mean flow in a quasi-frozen manner, i.e., the turbulent fluctuations evolve slowly compared to the mean velocity. This naturally restricts its application to low turbulence intensities. The second relation between temporal and spatial fluctuations has been developed by Kraichnan [3] and Tennekes [4] in terms of the so-called random sweeping hypothesis and is based on the assumption that the small-scale fluctuations in a turbulent flow are swept by the large-scale eddies in a random manner.

While a single-point measurement is not sufficient to decide which of these relations is valid for a given turbulent flow, multi-point measurements have the potential to determine the wavenumber-frequency turbulence spectrum without assuming Taylor's hypothesis or the random sweeping hypothesis. Multi-point measurements are available in various laboratory and geophysical turbulence studies, but are often limited in their statistical quality due to the challenges imposed by real-world turbulent flows. This motivates the construction of a simple model spectrum which contains both the effects of mean flow advection and random sweeping velocity as parameters. While modeling of wavenumber spectra has been largely discussed in the literature, see e.g. Davidson [5] and references therein, the joint consideration of frequencies and wavenumber is treated more rarely. Formulated in real space, this problem has been addressed recently in the framework of the so-called Elliptic Model (He and Zhang [6], Zhao and He [7]). In the Elliptic Model two-point–two-time velocity correlations are constructed such that the isocorrelation lines are ellipses parametrized by the mean and sweeping velocity, which leads to much better agreement with experimental and DNS data than the classic Taylor hypothesis. This gives further motivation to consider a simplified theoretical model in real and Fourier space.

Here we derive a simple model containing the mean flow velocity and the random sweeping velocity as free parameters, which is motivated by an idealized advection problem originally introduced by Kraichnan [3]. As a result the model spectrum consists of an instantaneous wavevector spectrum weighted by a Gaussian frequency distribution which includes the mean flow effects as a Doppler shift term and sweeping effects as a Doppler broadening. For power-law spectra the model has the interesting feature that the wavenumber spectrum and frequency spectrum exhibit the same spectral index, which leads to a $|\omega|^{-5/3}$ dependence of the frequency when a classical Kolmogorov scaling is assumed for the energy spectrum in wavenumber space, independent of the mean and sweeping velocity. We furthermore show that this

* mwilczek@uni-muenster.de

spectrum is consistent with the Elliptic Model recently introduced by He and coworkers [6, 7] and discuss its properties with respect to space-time correlations of the velocity.

II. INFLUENCE OF MEAN AND SWEEPING VELOCITY

A. Kraichnan's advection problem revisited

To understand the effects of sweeping and mean velocity on the wavenumber-frequency spectrum, we generalize a simple idealized advection problem originally discussed by Kraichnan [3]. In the following, we are interested in the statistical properties of a small-scale velocity field $\boldsymbol{u}$, which is swept by a large-scale velocity field $\boldsymbol{v}$. For the sake of simplicity, the field $\boldsymbol{u}$ is taken spatially varying, but constant in time. The sweeping velocity field $\boldsymbol{v}$ is also considered constant in time and, due to the large scale separation, also constant in space. However, the sweeping velocity is assumed to have a Gaussian ensemble distribution. Furthermore, the large and small-scale fields are assumed to be statistically independent initially. Additionally we take into account a constant mean flow, $\boldsymbol{v}_0$, which is the same for all members of the ensemble. As a result the total velocity field is given by $\boldsymbol{u}+\boldsymbol{v}_0+\boldsymbol{v}$. We now follow along the lines of Kraichnan [3] and assume that the small-scale turbulent velocity field is passively advected by the mean and sweeping velocities

$$\frac{\partial \boldsymbol{u}(\boldsymbol{k},t)}{\partial t} = -\mathrm{i}\left[\boldsymbol{k}\cdot(\boldsymbol{v}_0+\boldsymbol{v})\right]\,\boldsymbol{u}(\boldsymbol{k},t) \tag{1}$$

where $\boldsymbol{u}(\boldsymbol{k},t)$ is the Fourier transform of the velocity field from real space to wavevector space; the time dependence enters due to the advection by the mean and sweeping velocity. This advection equation is readily solved, yielding the expression for the Fourier coefficients

$$\boldsymbol{u}(\boldsymbol{k},t) = \exp\left[-\mathrm{i}\boldsymbol{k}\cdot(\boldsymbol{v}_0+\boldsymbol{v})t\right]\,\boldsymbol{u}(\boldsymbol{k},0)\,. \tag{2}$$

Based on this result we now connect the two-time energy spectrum $E(\boldsymbol{k},\tau)$ to the instantaneous energy spectrum $E(\boldsymbol{k})$, which is fully specified by the statistical properties of the velocity field $\boldsymbol{u}$ (see appendix A for a precise definition of the spectra). A straightforward calculation, which is detailed in appendix B, then yields

$$E(\boldsymbol{k},\tau) = E(\boldsymbol{k})\left\langle\,\exp\left[-\mathrm{i}\boldsymbol{k}\cdot(\boldsymbol{v}_0+\boldsymbol{v})\,\tau\right]\right\rangle \tag{3}$$

where $E(\boldsymbol{k}) = \Phi_{ii}(\boldsymbol{k})/2$ denotes the energy spectrum in the wavevector domain, defined as half the trace of the spectral energy tensor. It can also be noted that for $\tau = 0$ the two-time energy spectrum reduces to the instantaneous energy spectrum, $E(\boldsymbol{k},0) = E(\boldsymbol{k})$. The above expression can be evaluated further as we are assuming a Gaussian sweeping velocity field, which leads to

$$E(\boldsymbol{k},\tau) = E(\boldsymbol{k})\,\exp\left[-\mathrm{i}\boldsymbol{k}\cdot\boldsymbol{v}_0\tau\right]\,\left\langle\,\exp\left[-\mathrm{i}\boldsymbol{k}\cdot\boldsymbol{v}\,\tau\right]\right\rangle \tag{4}$$

$$= E(\boldsymbol{k})\exp\left[-\mathrm{i}\boldsymbol{k}\cdot\boldsymbol{v}_0\tau - \frac{\langle\boldsymbol{v}^2\rangle k^2\tau^2}{6}\right]. \tag{5}$$

For Eq. (4) we used the fact that the mean velocity is the same for all ensemble members and hence can be pulled out of the average. The averaging operation leading to Eq. (5) was evaluated under the above assumption of a Gaussian distributed sweeping velocity. For the case of vanishing mean flow, $\boldsymbol{v}_0 = \boldsymbol{0}$, the original random sweeping hypothesis introduced in [3] is recovered. In the presence of the mean velocity $\boldsymbol{v}_0$ the two-time energy spectrum is expressed as a combination of harmonic oscillation $\exp[-\mathrm{i}\boldsymbol{k}\cdot\boldsymbol{v}_0\,\tau]$ and exponential decay $\exp[-\alpha\tau^2]$ (where $\alpha = \langle\boldsymbol{v}^2\rangle k^2/6$). With this, the temporal correlations are fully specified. The (small-scale) energy spectrum in wavevector space $E(\boldsymbol{k})$, however, remains unspecified in these simple considerations and will be taken from classic turbulence theory as discussed below.

B. Wavenumber-frequency spectrum

To obtain the wavenumber-frequency spectrum, we note that Eq. (5) consists of the spectrum in wavevector space multiplied by the Fourier transform of a Gaussian distribution with mean velocity $\boldsymbol{U} = \boldsymbol{v}_0$ and a variance specified by the sweeping velocity $V = \sqrt{\langle\boldsymbol{v}^2\rangle/3}$. Hence the Fourier transform of Eq. (4) from the time to the frequency domain leads to a general expression for the wavenumber-frequency spectrum according to

$$\begin{aligned} E(\boldsymbol{k},\omega) &= \frac{1}{2\pi}\int \mathrm{d}\tau\, E(\boldsymbol{k},\tau)\,\exp[\mathrm{i}\omega\tau] \\ &= \frac{E(\boldsymbol{k})}{\sqrt{2\pi k^2V^2}}\exp\left[-\frac{(\omega-\boldsymbol{k}\cdot\boldsymbol{U})^2}{2k^2V^2}\right]. \end{aligned} \tag{6}$$

This clarifies that the mean velocity leads to a Doppler shift of frequencies whereas the sweeping velocity broadens the spectrum in the frequency domain. We emphasize that $\boldsymbol{U}$ and V are free parameters that can be determined from flow measurement. Although this result has been obtained for an idealized advection problem, the main features (Doppler shift due to mean flow and Doppler broadening due to sweeping effects) are expected to hold also for real turbulent flows.

The energy spectrum $E(\boldsymbol{k},\omega)$ may be anisotropic, either by anisotropy of the small-scale field $\boldsymbol{u}$ resulting in a wavevector anisotropy of $E(\boldsymbol{k})$ or by the term related to the Doppler shift $\boldsymbol{k}\cdot\boldsymbol{U}$. While the former is an intrinsic anisotropy of the physical system, the latter is rather a measurement effect that can be eliminated by Galilean transformation into the co-moving frame with the mean flow. It is worthwhile to note that Fung et al. [8] also derived a model spectrum in the wavenumber-frequency domain very similar to the one proposed here. Our model differs in that the frequency shift is solely by the Doppler shift imposed by the mean flow, while Fung et al. [8] assume that random sweeping affects both frequency shift and frequency broadening in the Gaussian distribution.

For the following discussion we assume that the small-scale velocity field $\boldsymbol{u}$ exhibits statistical isotropy, which

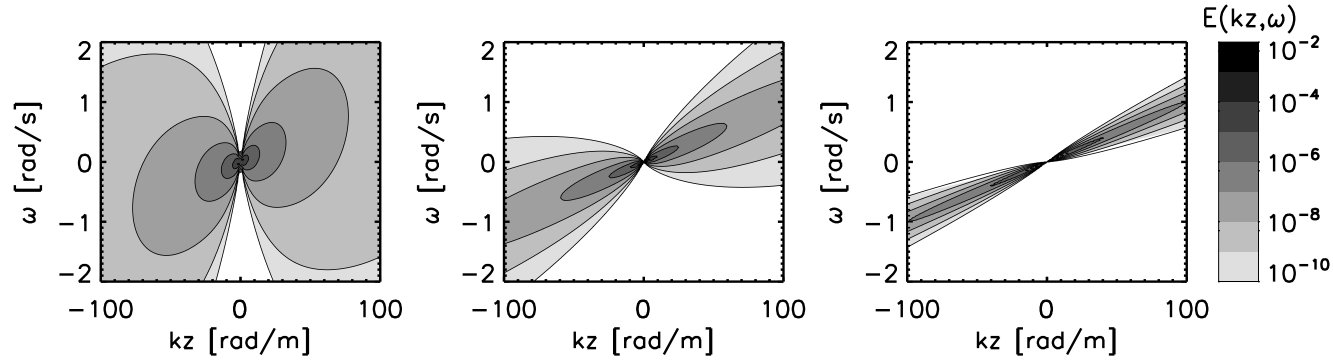

FIG. 1. Streamwise wavenumber-frequency spectrum for varying sweeping velocity for various ratios U/V of the mean to sweeping velocity, where the mean velocity is set to $U = 0.01\,\mathrm{m/s}$. Left: $U/V = 1.0$, middle: $U/V = 5.0$, right: $U/V = 20.0$. The units of the spectrum (contour scale bar) are $[E(k_z,\omega)] = \mathrm{m}^3\,\mathrm{s}^3$.

implies that the spectral tensor [9]

$$\Phi_{ij}(\boldsymbol{k}) = \frac{E(k)}{4\pi k^2}\left[\delta_{ij} - \frac{k_i k_j}{k^2}\right] \tag{7}$$

is fully determined by the energy spectrum $E(k)$, which then is a function of the modulus of the wavevector only. Applying Kolmogorov's similarity hypotheses [1] then leads to an expression for the inertial-range spectrum $E(k)$ for $E(\boldsymbol{k})$ in Eq. (6) according to

$$E(k) = C_{\mathrm{K}}\epsilon^{2/3}k^{-5/3} \tag{8}$$

with the energy transfer rate ϵ and the Kolmogorov constant C_{K}. Interestingly, the only directional dependence in Eq. (6) then comes from the Doppler shift term.

C. Graphical representation

The effects of the mean and sweeping velocities on the energy spectrum can be understood from a wavenumber-frequency diagram, especially enabling us to visualize the spectral transitions into the frozen-in flow approximation and the random sweeping approximation. For a graphical presentation it is useful to consider a mean flow in z-direction, $\boldsymbol{U} = U\boldsymbol{e}_z$ and reduce the wavenumber-frequency spectrum $E(\boldsymbol{k},\omega)$ to the streamwise wavenumber-frequency spectrum

$$E(k_z,\omega) = \int \mathrm{d}k_x \int \mathrm{d}k_y\, E(\boldsymbol{k},\omega) \tag{9}$$

where k_z denotes the streamwise wavenumber. In the following we assume the Kolmogorov spectrum (8) with $C_K = 1.5$. A fifth-order Newton-Cotes method is used for the numerical integration. Fig. 1 (left panel) displays an example of the streamwise spectrum in the ranges $|k_z| \leq 100\,\mathrm{rad/m}$ and $|\omega| \leq 2\,\mathrm{rad/s}$ for the energy dissipation rate $\epsilon = 1.0 \times 10^{-6}\,\mathrm{W/kg}$, the mean velocity $U = 0.01\,\mathrm{m/s}$ and the sweeping velocity $V = 0.01\,\mathrm{m/s}$. These values are typical for oceanic turbulence [10, 11]. The spectrum exhibits a reflection symmetry under the transformation $(k_z,\omega) \to (-k_z,-\omega)$. The spectral energy peaks at the origin due to the algebraic decay of the spectrum and has an elongation aligned with the Doppler shift imposed by the mean velocity $\omega = k_z U$.

To study the limiting case of Taylor's hypothesis, we keep the mean velocity $U = 0.01\,\mathrm{m/s}$ fixed and consider $U/V = 1.0$ (Fig. 1 left), $U/V = 5.0$ (Fig. 1 middle), and $U/V = 20.0$ (Fig. 1 right). The ratio of the mean to the sweeping velocity, U/V, can be used to judge the validity of frozen-in flow approximation such that larger values qualify a better approximation. The tilt of the spectral extension reflects the Doppler shift, which does not vary among the three cases. The frequency broadening, on the other hand, becomes smaller for increasing ratios of the mean to the sweeping velocity. In the limit of vanishing sweeping velocity ($V \to 0$) Taylor's frozen-in flow hypothesis is restored, and relabeling the frequency into wavenumber ($\omega^{-5/3} \to (kU)^{-5/3}$) is valid.

The other limit, vanishing mean velocity, is investigated in Fig. 2. The sweeping velocity is fixed to $V = 0.01\,\mathrm{m/s}$ as in the left panel of Fig. 1, and the spectrum is evaluated for the ratio $U/V = 2.0$ (Fig. 2 left); $U/V = 0.5$ (Fig. 2 middle); and $U/V = 0.0$ (Fig. 2 right). Because the sweeping velocity does not change, the frequency broadening is the same among the three spectra; but the Doppler shift or the tilt of the spectral extension is diminished with decreasing mean velocity. In the right panel of Fig. 2 the random sweeping approximation is restored, and the spectrum exhibits not only the reflection symmetry $(k_z,\omega) \to (-k_z,-\omega)$ but is also invariant under the transformations $(k_z,\omega) \to (-k_z,\omega)$ and $(k_z,\omega) \to (k_z,-\omega)$.

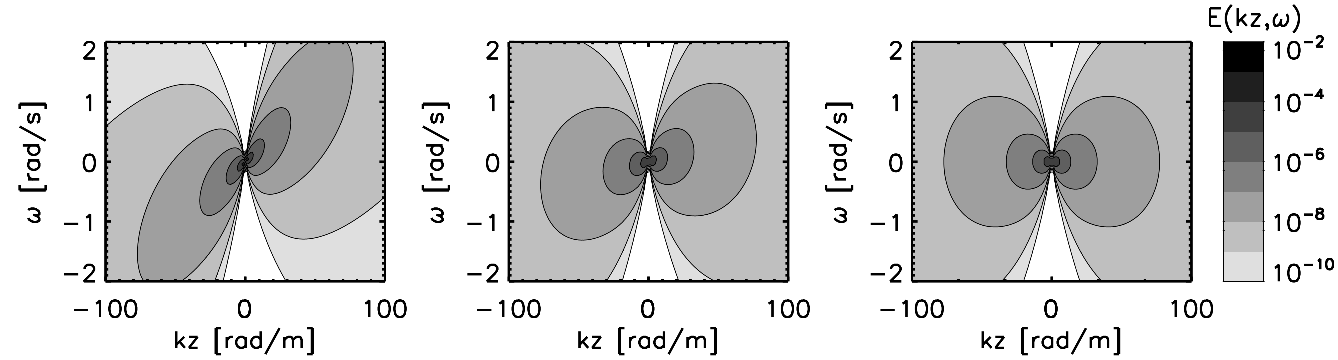

FIG. 2. Streamwise wavenumber-frequency spectrum for varying sweeping velocity for various ratios U/V of the mean to sweeping velocity, where the sweeping velocity is set to $V = 0.01\,\mathrm{m/s}$. Left: $U/V = 2.0$, middle: $U/V = 0.5$, right: $U/V = 0.0$.

III. PROPERTIES OF THE MODEL SPECTRUM

A. Eulerian wavenumber spectrum

The model spectrum (6) exhibits various interesting properties. First we check that the Eulerian wavenumber spectrum can be recovered from our model. To this end, we integrate over the frequency contribution

$$E(\boldsymbol{k}) = \int \mathrm{d}\omega \, E(\boldsymbol{k}, \omega) \tag{10}$$

which is a trivial task due to the Gaussian frequency contribution. To obtain the energy spectrum, we additionally integrate over solid angles yielding

$$E(k) = \int_0^{2\pi} \mathrm{d}\varphi \int_0^{\pi} \mathrm{d}\vartheta \, k^2 \sin\vartheta \, E(\boldsymbol{k}) = C_{\mathrm{K}} \epsilon^{2/3} k^{-5/3}. \tag{11}$$

That means, the frequency shift imposed by the Doppler effect $\boldsymbol{k}\cdot\boldsymbol{U}$ does not influence frequency integration, leaving the spectrum Eq. (11) invariant under a Galilean transformation. Hence the wavenumber spectrum should be independent from the choice of reference frame. The reduction to the wavenumber spectrum, of course, is a trivial consequence of the fact that our model spectrum is a product of the wavevector contribution with a Gaussian frequency contribution.

B. Eulerian frequency spectrum

Obtaining the Eulerian frequency contribution is a more involved task. To reduce to the frequency contribution, integration of the full wavevector space has to be performed. The result reads (see appendix C for a step-by-step evaluation)

$$E(\omega) = C(U, V) \, C_K \epsilon^{2/3} |\omega|^{-5/3} \tag{12}$$

where

$$C(U,V) = \int_0^{\infty} \mathrm{d}\gamma \, \frac{\gamma^{2/3}}{4U} \left[\mathrm{erf}\left(\frac{\gamma + U}{\sqrt{2}V} \right) - \mathrm{erf}\left(\frac{\gamma - U}{\sqrt{2}V} \right) \right] .$$

For this calculation we have assumed an infinitely extended inertial range, and we have chosen the coordinate system such that $\boldsymbol{U} = U\boldsymbol{e}_z$. Note that the term in brackets corresponds to a function localized around the origin with a width related to U and a steepness related to V, thus leading to a convergent integral. If we limit the inertial range and introduce a large-scale cutoff, $C(U, V)$ will also depend on ω introducing integral and dissipative effects also for the Eulerian frequency spectrum. An important feature of this result is that the frequency spectrum is given as a power-law with precisely the same spectral index as the Eulerian wavenumber spectrum, which is a direct consequence of the fact that the spectral broadening and the Doppler shift are linear functions of k. This, in turn, is the outcome of Kraichnan's idealized advection problem. It is furthermore noteworthy that the spectral index is independent of U and V, which has interesting implications for experimental observations. In turbulence experiments, the Eulerian wavenumber spectrum often is obtained from the Eulerian frequency spectrum by exploiting the Taylor hypothesis and neglecting sweeping effects. The reason why this yields satisfactory results is revealed by our simple model calculation: the spectral index is independent of the sweeping velocity! However, as the prefactor C depends on U and V. This has to be taken into account when determining the Kolmogorov constant from experimental single-point measurement.

We also verify the reduction property for our graphical example by integrating over the frequencies and wavenumbers, yielding the streamwise wavenumber spectrum $E(k_z)$ and the Eulerian frequency spectrum $E(\omega)$,

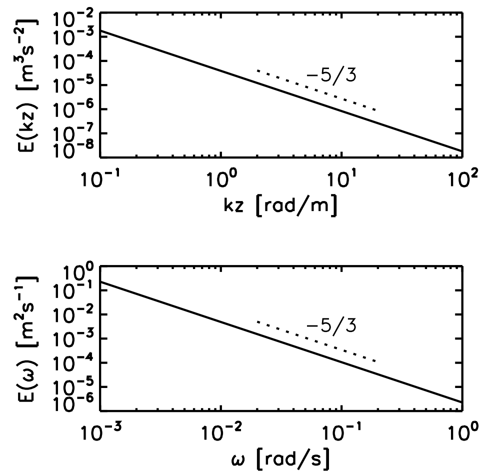

FIG. 3. Streamwise energy spectrum (upper panel) and frequency spectrum (lower panel) for the choice of parameters of Fig. 1, left panel.

respectively,

$$E(k_z) = \int \mathrm{d}\omega\, E(k_z, \omega) \tag{13}$$

$$E(\omega) = \int \mathrm{d}k_z\, E(k_z, \omega). \tag{14}$$

Integrals are again evaluated numerically using the fifth-order Newton-Cotes method. As can be seen in Fig. 3 both the streamwise energy spectrum $E(k_z)$ and the frequency spectrum $E(\omega)$ exhibit a power-law with the spectral index $-5/3$, confirming the above analytical result.

C. Space-time correlations and the relation to the Elliptic Model

To conclude the discussion of the properties of the model spectrum, we would like to connect our results to the Elliptic Model introduced by He and co-workers [6, 7]. In [7] a turbulent shear flow has been considered and the streamwise space-time correlation

$$R(r,\tau) = \langle \boldsymbol{u}(\boldsymbol{x}, t) \cdot \boldsymbol{u}(\boldsymbol{x} + r\boldsymbol{e}_z, t + \tau)\rangle \tag{15}$$

has been investigated. Here and in the following we assume the mean flow again to point into z-direction, $\boldsymbol{U} = U\boldsymbol{e}_z$. The isocorrelation lines of the space-time correlation are defined by

$$R(r,\tau) = R(r_\mathrm{E}, 0)\,. \tag{16}$$

With the aim to generalize Taylor's hypothesis and motivated by experimental and DNS results, it was proposed that r_E specifies ellipses depending on the mean and sweeping velocity

$$r_\mathrm{E}^2 = (r - U_\mathrm{E}\tau)^2 + V_\mathrm{E}^2\tau^2\,. \tag{17}$$

In the original paper U_E and V_E have been obtained by a second-order Taylor expansion of the streamwise correlation function according to

$$U_\mathrm{E} = -\frac{R_{r\tau}}{R_{rr}} \qquad \text{and} \qquad V_\mathrm{E}^2 = \frac{R_{\tau\tau}}{R_{rr}} - U_\mathrm{E}^2 \tag{18}$$

with $R_{rr} = \frac{\partial^2 R}{\partial r^2}(0,0)$, $R_{r\tau} = \frac{\partial^2 R}{\partial r \partial \tau}(0,0)$ and $R_{\tau\tau} = \frac{\partial^2 R}{\partial \tau^2}(0,0)$.

It turns out that our model spectrum is related to the Elliptic Model in a straightforward manner. However, we here do not take into account shear in the mean flow but only the effects of mean and sweeping velocity. The velocity correlation (or covariance) is obtained from our model spectrum by (see also appendix A for the definition of the two-point–two-time velocity covariance tensor)

$$R(r,\tau) = R_{ii}(r\boldsymbol{e}_z, \tau) = 2\int \mathrm{d}\boldsymbol{k}\,\mathrm{d}\omega\, E(\boldsymbol{k}, \omega)\, \exp[\mathrm{i}(k_z r - \omega\tau)]\,. \tag{19}$$

With this relation, we can also calculate the Taylor coefficients from our model Eq. (6) yielding

$$\begin{aligned} R_{rr} &= -2\int \mathrm{d}\boldsymbol{k}\,\mathrm{d}\omega\, k_z^2\, E(\boldsymbol{k}, \omega) \\ &= -\frac{2}{3}\int \mathrm{d}k\, k^2\, E(k) \end{aligned} \tag{20}$$

$$\begin{aligned} R_{r\tau} &= 2\int \mathrm{d}\boldsymbol{k}\,\mathrm{d}\omega\, k_z\,\omega\, E(\boldsymbol{k}, \omega) \\ &= \frac{2}{3}U\int \mathrm{d}k\, k^2\, E(k) \end{aligned} \tag{21}$$

$$\begin{aligned} R_{\tau\tau} &= -2\int \mathrm{d}\boldsymbol{k}\,\mathrm{d}\omega\, \omega^2\, E(\boldsymbol{k}, \omega) \\ &= \left(-2V^2 - \frac{2}{3}U^2\right)\int \mathrm{d}k\, k^2\, E(k)\,. \end{aligned} \tag{22}$$

This leads us to the result

$$U = -\frac{R_{r\tau}}{R_{rr}} \qquad \text{and} \qquad 3V^2 = \frac{R_{\tau\tau}}{R_{rr}} - U^2 \tag{23}$$

which is almost identical to the definitions (18). The additional factor 3 comes due to the fact that we have defined V as the standard deviation of a single component of the sweeping velocity field. As in our model U and V by construction are the mean and sweeping velocities, this result confirms the physical interpretation of the parameters U_E and V_E of the Elliptic Model.

Next we derive a relation between the streamwise velocity correlation function and the energy spectrum. To this end we consider

$$R(r,\tau) = R_{ii}(r\boldsymbol{e}_z, \tau) = 2\int \mathrm{d}\boldsymbol{k}\, E(\boldsymbol{k}, \tau)\, \exp[\mathrm{i}k_z r]\,. \tag{24}$$

Now inserting our model Eq. (5) and assuming an isotropic small-scale velocity field we obtain

$$R(r,\tau) = 2\int \mathrm{d}k\, E(k)\, \frac{\sin[k(r - U\tau)]}{k(r - U\tau)}\, \exp\left[-\frac{1}{2}k^2V^2\tau^2\right]. \tag{25}$$

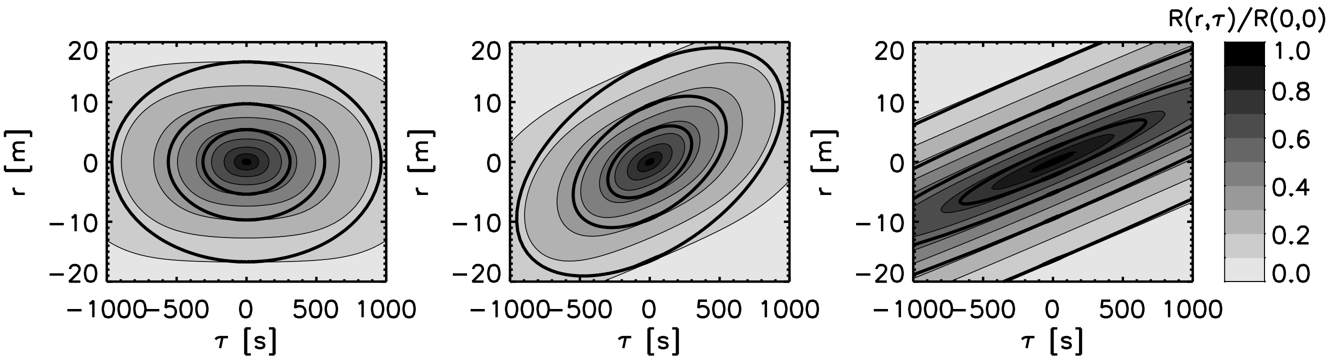

FIG. 4. Streamwise space-time correlation evaluated from Eq. (25) in the wavenumber range from 0.1 rad/m to 100.0 rad/m for three cases: $U = 0.0$ m/s and $V = 0.01$ m/s (left panel); $U = V = 0.01$ m/s (middle panel); and $U = 0.01$ m/s and $V = 0.002$ m/s (right panel). The solid black lines define the isocorrelation lines (27) of the elliptic model.

For a given model energy spectrum the space-time correlation is hereby fully specified. In general the last integration now can be performed numerically. The relation of our model spectrum to the Elliptic Model can still be pursued further. Evaluating relation (16) leads to the condition for the isocorrelation lines of our model:

$$\int \mathrm{d}k\, E(k)\, \frac{\sin\left[k(r-U\tau)\right]}{k(r-U\tau)}\, \exp\left[-\frac{1}{2}k^2V^2\tau^2\right] = \int \mathrm{d}k\, E(k)\, \frac{\sin kr_E}{kr_E} \tag{26}$$

While this relation cannot be solved for r_E analytically, a second-order Taylor expansion of the integrands leads to

$$r_E^2 = (r-U\tau)^2 + 3V^2\tau^2 \tag{27}$$

which is precisely the starting point of the Elliptic Model. Hence our calculations give further theoretical justification for the Elliptic Model. Because this result is obtained as a second-order approximation, it is also interesting to compare the ellipses defined by Eq. (27) to the isocorrelation lines of our model. This is shown in Fig. 4 for a spectrum which is chosen to obey $E(k) \sim k^{-5/3}$ in the inertial range from $k = 0.1$ rad/m to $k = 100.0$ rad/m and vanishing elsewhere for three different parameter sets: $U = 0.0$ m/s and $V = 0.01$ m/s (Fig. 4 left, random sweeping approximation); $U = V = 0.01$ m/s (Fig. 4 middle); and $U = 0.01$ m/s and $V = 0.002$ m/s (Fig. 4 right, close to frozen-in flow approximation). As expected for a low-order approximation, in all three cases the elliptic model compares satisfactory to the isocorrelation lines of our model for small temporal and spatial distances. For larger distances, however, systematic deviations become apparent especially for small ratios of mean and sweeping velocities. This is especially visible for the case where mean and sweeping velocity are identical (Fig. 4 middle), where our model predicts clearly non-elliptical and asymmetric isocorrelation lines. The agreement of the two models becomes better for increasing ratios of mean and sweeping velocities. Because the elliptic model can be regarded as a higher-order improvement of Taylor's hypothesis, it is evident that a better agreement occurs with increasing ratio of mean and sweeping velocity, as can be seen in Fig. 4 (right). We would like to stress, though, that it is not evident at this stage which of the models yields a more accurate description of turbulent flows. A comparison to experimental or DNS data as presented in [12–15] as well as an investigation of different choices of model wavenumber spectra is a possible direction for future work.

IV. SUMMARY AND DISCUSSION

By extending a simple advection problem initially proposed by Kraichnan [3], we derived a simple model spectrum in the wavenumber-frequency domain including the mean and sweeping velocity in a natural way. The model spectrum consists of an instantaneous spectrum in the wavevector domain multiplied by Gaussian frequency distribution. The mean value of this distribution depends on the mean flow velocity and induces a Doppler shift, whereas the variance is specified by the random sweeping velocity inducing a frequency broadening.

The spectrum is reduced either to the wavenumber or to the frequency spectrum by integration. Provided the energy spectrum in wavenumber space has a power-law dependence, the model has the interesting property that the frequency spectrum exhibits the same spectral index, independent of the mean and sweeping velocities. As our calculations show, this is a simple consequence of the fact that the Doppler shift and frequency broadening are linear functions of the wavenumber. Opposed to this invariance of the spectral index the prefactor of the spectrum is found to depend on the mean and sweeping velocities.

These results have interesting consequences for measurements of turbulent flows: Due to the independence of the spectral index of the mean and sweeping velocity, it is not possible to determine the wavenumber-frequency spectrum uniquely from measurement of either the wavenumber or frequency spectrum without knowledge of the characteristic velocities (U and V). The wavenumber-frequency spectrum is accessible only by proper multi-point measurements that allow us to distinguish between temporal and spatial fluctuations. Moreover, once the two characteristic velocities are available from multi-point measurements, our model can be used for a low-dimensional parametrization of a full wavenumber-frequency spectrum.

It is worth mentioning that the determination of the characteristic velocities might also be possible from spatial-temporal sampling of data other than velocity, for example from measurement of density or temperature variation (assuming passive scalar model), providing an independent method of velocity measurements.

We have also discussed the implications of our model spectrum for the two-point–two-time velocity correlations, which are obtained by Fourier transform. As expected, the space-time correlations decay with increasing temporal and spatial separation leading to approximately elliptical isocorrelation lines. The model spectrum has also been shown to be closely related to the recently introduced Elliptic Model. In particular we have shown that the assumptions underlying the Elliptic Model can be derived from our simple model giving further theoretical justification.

In Ref. [16] the random sweeping hypothesis has been used to evaluate time correlations of the pressure field. A possible generalization of these calculations to the case of additional mean flow remains an interesting future application of the current model.

ACKNOWLEDGMENTS

We would like to thank Guowei He, Haitao Xu, and the referees for constructive comments. This work was financially supported by the Bundesministerium für Wirtschaft und Technologie and the Deutsches Zentrum für Luft- und Raumfahrt, Germany, under contract 50 OC 0901, and Collaborative Research Center 963, "Astrophysical Flow, Instabilities, and Turbulence" of German Science Foundation. This research was also supported in part by the National Science Foundation under Grant No. NSF PHY11-25915.

[1] A. N. Kolmogorov, Dokl. Akad. Nauk SSSR **30**, 299 (1941).
[2] G. I. Taylor, P. Roy. Soc. Lond. A Mat. **164**, 476 (1938).
[3] R. H. Kraichnan, Phys. Fluids **7**, 1723 (1964).
[4] H. Tennekes, J. Fluid Mech. **67**, 561 (1975).
[5] P. A. Davidson, *Turbulence - An Introduction for Scientists and Engineers* (Oxford University Press, Oxford, England, 2004).
[6] G.-W. He and J.-B. Zhang, Phys. Rev. E **73**, 055303 (2006).
[7] X. Zhao and G.-W. He, Phys. Rev. E **79**, 046316 (2009).
[8] J. C. H. Fung, J. C. R. Hunt, N. A. Malik, and R. J. Perkins, J. Fluid Mech. **236**, 281 (1992).
[9] G. K. Batchelor, *The theory of homogeneous turbulence* (Cambridge University Press, Cambridge, England, 1953).
[10] R.-C. Lien, E.-A. D'Asaro, and G. T. Dairiki, J. Fluid Mech. **362**, 177 (1998).
[11] R.-C. Lien and E.-A. D'Asaro, J. Atmos. Oceanic Technol. **23**, 964 (2006).
[12] J. A. B. Wills, J. Fluid Mech. **20**, 417 (1964).
[13] H. Choi and P. Moin, Phys. Fluids A **2**, 1450 (1990).
[14] J. Kim and F. Hussain, Phys. Fluids A **5**, 695 (1993).
[15] X. He and P. Tong, Phys. Rev. E **83**, 037302 (2011).
[16] H.-D. Yao, G.-W. He, M. Wang, and X. Zhang, Phys. Fluids **20**, 025105 (2008).

Appendix A: Notation and conventions

This section shall give a brief overview of the notation and conventions used in this paper. We introduce the Fourier transform of the velocity field according to

$$\boldsymbol{u}(\boldsymbol{x},t) = \int \mathrm{d}\boldsymbol{k}\, \boldsymbol{u}(\boldsymbol{k},t)\, \exp[\mathrm{i}\boldsymbol{k}\cdot\boldsymbol{x}] \tag{A1}$$

$$\boldsymbol{u}(\boldsymbol{k},t) = \frac{1}{(2\pi)^3}\int \mathrm{d}\boldsymbol{x}\, \boldsymbol{u}(\boldsymbol{x},t)\, \exp[-\mathrm{i}\boldsymbol{k}\cdot\boldsymbol{x}]\,. \tag{A2}$$

In the following, we will consider statistically stationary and homogeneous turbulence, which implies that two-point quantities depend only on the distance vector $\boldsymbol{r}$, and two-time quantities depend only on the time lag τ.

In the literature, the two-point–one-time velocity covariance tensor for turbulence usually is defined as (see e.g. [9])

$$R_{ij}(\boldsymbol{r}) = \langle u_i(\boldsymbol{x},t)\, u_j(\boldsymbol{x}+\boldsymbol{r},t)\rangle\,. \tag{A3}$$

Its Fourier transform, the so-called energy spectrum tensor, is defined as

$$\Phi_{ij}(\boldsymbol{k}) = \frac{1}{(2\pi)^3}\int \mathrm{d}\boldsymbol{r}\, R_{ij}(\boldsymbol{r})\, \exp[-\mathrm{i}\boldsymbol{k}\cdot\boldsymbol{r}]\,. \tag{A4}$$

The inverse relation simply reads

$$R_{ij}(\boldsymbol{r}) = \int \mathrm{d}\boldsymbol{k}\, \Phi_{ij}(\boldsymbol{k})\, \exp[\mathrm{i}\boldsymbol{k}\cdot\boldsymbol{r}]\,. \tag{A5}$$

The kinetic energy per Fourier coefficient can simply be obtained from the energy spectrum tensor by

$$E(\boldsymbol{k}) = \frac{\Phi_{ii}(\boldsymbol{k})}{2}\,. \tag{A6}$$

We will refer to this quantity as the instantaneous energy spectrum. Up to now, only single-time quantities have been considered. To generalize these considerations to the two-time case, we define the two-point–two-time velocity covariance tensor

$$R_{ij}(\boldsymbol{r},\tau) = \langle u_i(\boldsymbol{x},t)\, u_j(\boldsymbol{x}+\boldsymbol{r},t+\tau)\rangle \tag{A7}$$

and its Fourier transform to wavevector space

$$\Phi_{ij}(\boldsymbol{k},\tau) = \frac{1}{(2\pi)^3}\int \mathrm{d}\boldsymbol{r}\, R_{ij}(\boldsymbol{r},\tau)\, \exp[-\mathrm{i}\boldsymbol{k}\cdot\boldsymbol{r}]\,. \tag{A8}$$

Relation (A6) can be generalized in the same manner to

$$E(\boldsymbol{k},\tau) = \frac{\Phi_{ii}(\boldsymbol{k},\tau)}{2}\,, \tag{A9}$$

which will be called two-time energy spectrum. As becomes clear from these definitions, the two-time quantities are distinguished from the one-time quantities by an additional argument only. The energy spectrum in the wavenumber-frequency domain is then obtained by

$$E(\boldsymbol{k},\omega) = \frac{1}{2\pi}\int \mathrm{d}\tau\, E(\boldsymbol{k},\tau)\, \exp[\mathrm{i}\omega\tau] \tag{A10}$$

with the inverse transform

$$E(\boldsymbol{k},\tau) = \int \mathrm{d}\omega\, E(\boldsymbol{k},\omega)\, \exp[-\mathrm{i}\omega\tau]\,. \tag{A11}$$

Compared to the definitions (A4)-(A5) we have defined the Fourier transform with opposite sign, which is physically consistent with an expansion into forward propagating waves along the wavevector $\boldsymbol{k}$.

Appendix B: Covariance of Fourier coefficients

To derive a relation between the two-time energy spectrum and the instantaneous energy spectrum for Kraichnan's advection problem, it is convenient to first calculate the covariance of two arbitrary Fourier coefficients and then establish a connection of the one-time and two-time spectral energy tensors. To this end we make use of Eq. (A2) and consider:

$$\langle u_i(\boldsymbol{k},t)\, u_j(\boldsymbol{k}',t')\rangle = \frac{1}{(2\pi)^6}\int \mathrm{d}\boldsymbol{x}\,\mathrm{d}\boldsymbol{x}'\,\langle u_i(\boldsymbol{x},t)\, u_j(\boldsymbol{x}',t')\rangle\, \exp[-\mathrm{i}(\boldsymbol{k}\cdot\boldsymbol{x}+\boldsymbol{k}'\cdot\boldsymbol{x}')] \tag{B1}$$

We now set $t' = t+\tau$ and $\boldsymbol{x}' = \boldsymbol{x}+\boldsymbol{r}$. Due to homogeneity, the two-point–two-time velocity covariance is independent of $\boldsymbol{x}$ and hence can be pulled out of the $\boldsymbol{x}$-integration. Additionally we note that

$$\delta(\boldsymbol{k}+\boldsymbol{k}') = \frac{1}{(2\pi)^3}\int \mathrm{d}\boldsymbol{x}\, \exp[-\mathrm{i}(\boldsymbol{k}+\boldsymbol{k}')\cdot\boldsymbol{x}]\,. \tag{B2}$$

This connects the covariance of the Fourier coefficients to the two-point–two-time velocity covariance tensor and its Fourier transform, the two-time spectral energy tensor,

$$\langle u_i(\boldsymbol{k},t)\, u_j(\boldsymbol{k}',t+\tau)\rangle = \frac{\delta(\boldsymbol{k}+\boldsymbol{k}')}{(2\pi)^3}\int \mathrm{d}\boldsymbol{r}\, R_{ij}(\boldsymbol{r},\tau)\, \exp[-\mathrm{i}\boldsymbol{k}'\cdot\boldsymbol{r}] = \delta(\boldsymbol{k}+\boldsymbol{k}')\,\Phi_{ij}(\boldsymbol{k}',\tau)\,. \tag{B3}$$

For $\tau = 0$ this relation reduces to corresponding single-time relation.

For Kraichnan's advection problem the two-time and single-time covariances are connected in a specifically simple manner. By insertion of the solution (2) we obtain

$$\begin{aligned}\big\langle u_i(\boldsymbol{k},t)\, u_j(\boldsymbol{k}',t+\tau)\big\rangle &= \big\langle u_i(\boldsymbol{k},0)\, u_j(\boldsymbol{k}',0)\, \exp\left[-\mathrm{i}\boldsymbol{k}\cdot(\boldsymbol{v}_0+\boldsymbol{v})t - \mathrm{i}\boldsymbol{k}'\cdot(\boldsymbol{v}_0+\boldsymbol{v})(t+\tau)\right]\big\rangle \\ &= \big\langle u_i(\boldsymbol{k},0)\, u_j(\boldsymbol{k}',0)\big\rangle\big\langle \exp\left[-\mathrm{i}\boldsymbol{k}\cdot(\boldsymbol{v}_0+\boldsymbol{v})t - \mathrm{i}\boldsymbol{k}'\cdot(\boldsymbol{v}_0+\boldsymbol{v})(t+\tau)\right]\big\rangle\end{aligned} \tag{B4}$$

where the second equality comes from the fact that the small-scale velocity field $\boldsymbol{u}$ and the sweeping velocity field $\boldsymbol{v}$ are statistically independent initially. In terms of the spectral energy tensors this relation takes the form

$$\delta(\boldsymbol{k}+\boldsymbol{k}')\,\Phi_{ij}(\boldsymbol{k}',\tau) = \delta(\boldsymbol{k}+\boldsymbol{k}')\,\Phi_{ij}(\boldsymbol{k}')\,\big\langle \exp\left[-\mathrm{i}\boldsymbol{k}\cdot(\boldsymbol{v}_0+\boldsymbol{v})t - \mathrm{i}\boldsymbol{k}'\cdot(\boldsymbol{v}_0+\boldsymbol{v})(t+\tau)\right]\big\rangle\,. \tag{B5}$$

Integration over $\boldsymbol{k}'$ lets us eliminate the delta functions and finally yields

$$\Phi_{ij}(\boldsymbol{k},\tau) = \Phi_{ij}(\boldsymbol{k})\,\big\langle \exp\left[-\mathrm{i}\boldsymbol{k}\cdot(\boldsymbol{v}_0+\boldsymbol{v})\,\tau\right]\big\rangle\,, \tag{B6}$$

which especially implies the desired result

$$E(\boldsymbol{k},\tau) = E(\boldsymbol{k})\,\big\langle \exp\left[-\mathrm{i}\boldsymbol{k}\cdot(\boldsymbol{v}_0+\boldsymbol{v})\,\tau\right]\big\rangle\,. \tag{B7}$$

Appendix C: Calculation of the frequency spectrum

The frequency spectrum is obtained from the wavenumber-frequency spectrum by integration of the wavevector. A step-by-step evaluation yields

$$E(\omega) = \int \mathrm{d}\boldsymbol{k}\, E(\boldsymbol{k},\omega) = \int \mathrm{d}\boldsymbol{k}\, \frac{E(\boldsymbol{k})}{\sqrt{2\pi k^2 V^2}} \exp\left[-\frac{(\omega - \boldsymbol{k}\cdot\boldsymbol{U})^2}{2k^2V^2}\right] \tag{C1}$$

$$= \int_0^\infty \mathrm{d}k \int_0^{2\pi} \mathrm{d}\varphi \int_0^\pi \mathrm{d}\vartheta\, \sin\vartheta\, \frac{C_\mathrm{K}\epsilon^{2/3}k^{-8/3}}{4\pi\sqrt{2\pi V^2}} \exp\left[-\frac{(\omega - kU\cos\vartheta)^2}{2k^2V^2}\right] \tag{C2}$$

$$= \int_0^\infty \mathrm{d}k\, \frac{C_\mathrm{K}\epsilon^{2/3}k^{-8/3}}{4U} \left[\mathrm{erf}\left(\frac{\omega + kU}{\sqrt{2}kV}\right) - \mathrm{erf}\left(\frac{\omega - kU}{\sqrt{2}kV}\right)\right] \tag{C3}$$

$$\overset{\gamma=\omega/k}{=} |\omega|^{-5/3} \int_0^\infty \mathrm{d}\gamma\, \frac{C_\mathrm{K}\epsilon^{2/3}\gamma^{2/3}}{4U} \left[\mathrm{erf}\left(\frac{\gamma + U}{\sqrt{2}V}\right) - \mathrm{erf}\left(\frac{\gamma - U}{\sqrt{2}V}\right)\right] \tag{C4}$$

$$= C(U,V)\, C_K \epsilon^{2/3}|\omega|^{-5/3} \tag{C5}$$

where

$$C(U,V) = \int_0^\infty \mathrm{d}\gamma\, \frac{\gamma^{2/3}}{4U} \left[\mathrm{erf}\left(\frac{\gamma + U}{\sqrt{2}V}\right) - \mathrm{erf}\left(\frac{\gamma - U}{\sqrt{2}V}\right)\right].$$

For this calculation we have assumed an infinitely extended inertial range, and we have chosen the coordinate system such that $\boldsymbol{U} = U\boldsymbol{e}_z$. If we limit the inertial range and introduce a large-scale cutoff, $C(U,V)$ will also depend on ω introducing integral and dissipative effects also for the Eulerian frequency spectrum.